Light emission from Na/Cu(111) induced by a scanning tunneling microscope

Peter Johansson
Department of Natural Sciences, University of Örebro, S–701 82 Örebro, Sweden

Germar Hoffmann and Richard Berndt
Institut für Experimentelle und Angewandte Physik, Christian-Albrechts-Universität zu Kiel, D–24098 Kiel, Germany
(Received 6 August 2002; published 20 December 2002)

Measurements of light emission from a scanning tunneling microscope probing a Na overlayer on the (111) surface of Cu are reported along with the results of a model calculation that essentially agree with the experimental ones. The observed light-emission spectra show two characteristic features depending on the bias voltage. When the bias voltage is smaller than the energy of the second quantum well state formed outside the Na overlayer the light emission is due to a plasmon-mediated process, while for larger biases light emission is mainly caused by quantum well transitions between the two levels.

DOI: 10.1103/PhysRevB.66.245415 PACS number(s): 73.20.At, 68.37.Ef, 73.20.Mf, 73.21.Fg

I. INTRODUCTION

The formation of quantum-well states (QWS) near the Fermi level is a characteristic feature of the electronic structure of alkali overlayers on the (111) surfaces of noble metals.[1–6] In these systems electrons may be confined to a narrow surface region; they cannot escape from the surface because of the vacuum barrier, and at the same time they cannot propagate into the noble metal because the periodic potential in the bulk creates a local band gap near the L point of the Brillouin zone. Alkali overlayers thus offer an interesting opportunity to study confined electron systems in metals and they have attracted considerable interest.

Up to now, most investigations of alkali overlayers have been carried out using photoemission spectroscopy, inverse photoemission spectroscopy and two-photon photoemission.[2,7–10] Thus the energies of the quantum-well states have been studied as a function of substrate and overlayer material as well as overlayer thickness (or coverage). In addition to measuring the position in energy of the quantum-well states, the lifetimes of these states have also been addressed.[11–13] The quantum-well states overlap in energy and space with three-dimensional states, producing interesting possibilities for quasiparticle decay to proceed simultaneously through both two- and three-dimensional channels as well as electron-phonon scattering.

In a recent experiment the system Na/Cu(111) was studied with an alternative experimental technique, light emission induced by electron injection from the tip of a scanning tunneling microscope (STM).[14] This technique has previously been used in studies of quite a few systems, most notably noble-metal surfaces and semiconductors.[15] In those cases photons are generated by a fraction of the tunneling electrons that undergo inelastic tunneling processes in which an amount of energy, limited to eU with U the bias voltage, is transferred from the electron to the photon. If the substrate is metallic, the rate of spontaneous light emission is increased compared with the case of inverse photoemission from an isolated surface.[16–25] This is due to enhanced vacuum fluctuations of the electromagnetic field in the tunnel gap between tip and sample as a result of the formation of localized interface-plasmon modes there. For semiconductor samples, on the other hand, electromagnetic effects are less important, instead the light emission is due to interband transitions in the semiconductor.[26,27] The STM tip serves to locally inject or generate minority charge carriers which then recombine with majority carriers giving rise to luminescence. Similar studies have also been carried out on semiconductor surfaces,[28,29] semiconductor quantum-wells[30] and quantum dots,[31] and adsorbed molecules.[32,33]

Interestingly enough, the light emission from Na/Cu(111) reported in Ref. 14, appears to involve both mechanisms described above. For a wide range of coverages, Na on Cu(111) exhibits several QWS. The lowest one, QWS1, has an energy close to the Fermi level (see Table I). At the coverages to be discussed below, it is either occupied or unoccupied. The other state, QWS2, lies well above the Fermi energy. As long as the bias voltage is low enough that electrons cannot be injected into QWS2 light emission is still possible, and it proceeds through the same ''plasmon-mediated'' mechanism as in the case of clean noble-metal surfaces. In this case electrons undergo an inelastic transition from a filled state in the tip to the empty QWS1 and a photon is emitted. This gives a fairly broad peak in the light-emission spectrum. Once the bias voltage is high enough that electrons can be injected directly into the upper quantum-well state (QWS2) the emission mechanism changes. A large part of the tunnel current will now go through QWS2, and light emission will mainly be due to transitions between QWS2 and QWS1, yielding a fairly sharply peaked spectrum. Of course, since the QWS wave functions are to a large extent confined to the region of space between the tip and

TABLE I. Energies of quantum-well states of Na on Cu(111) in eV relative to the Fermi energy E_F as obtained from tunneling spectroscopy of the differential conductance. At a coverage of 1 ML, the lowest state is occupied ($E_1<0$).

	0.6 ML	1 ML	2 ML
E_1	0.4	−0.15	0.15
E_2	2.05	2.3	2.2

sample, the light-emission rate is still enhanced by the electromagnetic fluctuations there.

In this paper we will support the scenario outlined above by model calculations that lead to very good qualitative agreement between experiment and theory. We will also present additional experimental results.

The rest of the paper is organized in the following way. In Sec. II we outline the experimental setup, and the experimental results are presented in Sec. III. Section IV gives a comprehensive description of the model calculation that we have carried out. Then in Sec. V, we compare theoretical and experimental results and discuss the implications. The paper is summarized in Sec. VI. Finally, an Appendix presents a derivation of the rate of light emission based on the Keldysh nonequilibrium Green's-function technique.

II. EXPERIMENTAL DETAILS

The experiments were performed with an ultrahigh vacuum (UHV) STM operated at a temperature $T=4.6$ K.[34] Photons in the energy range 1.2 eV$<h\nu<$3.5 eV were detected with a lens system in UHV coupling the light to a grating spectrometer and a liquid-nitrogen-cooled charge-coupled device camera.[35] All spectra have been corrected for the wavelength-dependent detection efficiency. Throughout the measurements it was verified that the surface structure was not modified during data acquisition.

W tips were prepared by electrochemical etching and subsequent sputtering and annealing in UHV. The Cu(111) surface was cleaned by repeated cycles of Ar-ion bombardment and annealing. Na films were evaporated from outgassed SAES Getters sources onto the Cu crystal held at room temperature. A quartz-crystal microbalance was used to estimate the coverage Θ which was further calibrated by the known binding energies of the quantum-well states.[2,7–10] After preparation at room temperature the sample was transferred to the STM and cooled to $T=4.6$ K.

Following Ref. 36 we define 1 ML as the most densely packed structure of the first Na layer, namely a $(3/2\times3/2)$ mesh. This pattern corresponds to four Na atoms per nine first-layer Cu atoms.

III. EXPERIMENTAL RESULTS

Figure 1 shows fluorescence spectra recorded over a range of sample voltages U from Cu(111) covered with 1 ML of Na. The emission from these surfaces is comprised of two distinct components. First, there is an emission band which is most clearly observed at low U. Its maximum shifts linearly to higher energies as U is increased. This emission is similar to the plasmon-mediated emission observed from noble-metal surfaces due to inelastic tunneling processes.[17–19,21,37]

A new spectral structure, the position of which only weakly depends on the sample voltage U, emerges at $h\nu=2.4$ eV when the bias is raised to $U\gtrsim2.5$ V. From its intensity, assuming isotropic emission, a quantum efficiency of approximately 10^{-5} photons per electron is estimated which is higher than typical values for conventional inverse photoelectron spectroscopy.

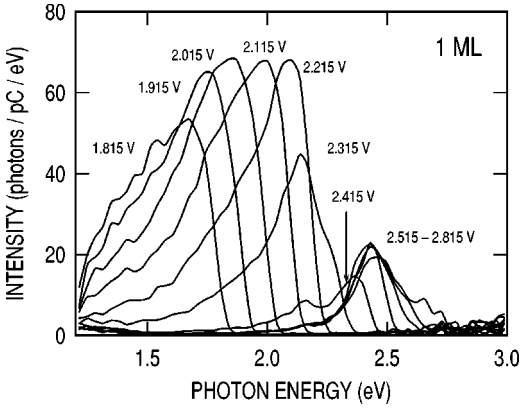

FIG. 1. Light-emission spectra of 1 ML Na measured for a series of sample voltages between 1.815 V and 2.815 V with a tunneling current of 10 nA. Small apparent undulations at low ($\lesssim1.6$ eV) and high ($\gtrsim2.6$ eV) photon energies are due to counting statistics. There is a qualitative change once the voltage reaches ≈2.5 V: Below, the peak emission shifts with the sample voltage; above, the emission maximum remains at $h\nu\approx2.4$ eV.

Qualitatively similar observations were made at other coverages (Fig. 2). In addition to a plasmon-related emission (circles) at low bias voltages we find emission (dots) at higher photon energies which are almost independent of the applied sample voltages. The positions of these emission features vary with the Na coverage: $h\nu$

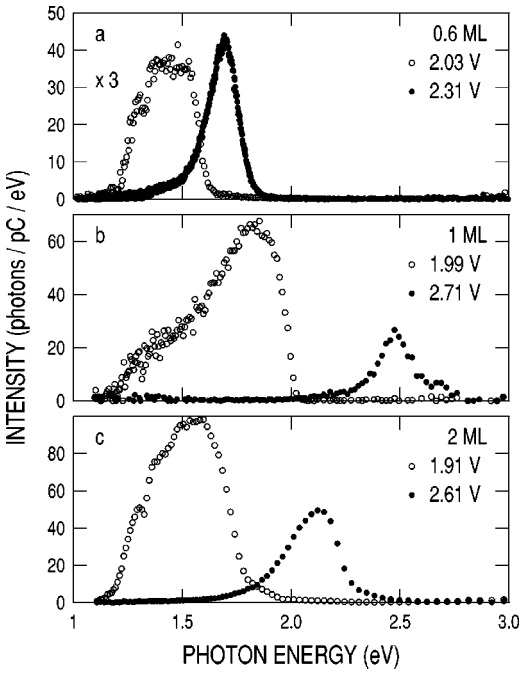

FIG. 2. Characteristic spectra obtained with a low sample voltage (circles) for which injection of electrons into the upper quantum-well state is not possible, and a high sample voltage (dots) where electrons can be injected into the upper QWS. The three panels display results from samples covered by 0.6, 1, and 2 ML of Na. A small dip of the intensity at ≈1.3 eV is due to a sharp absorption of the optical fiber used in the experiment, which is not fully corrected for.

~1.7, 2.5, and 2.1 eV at coverages 0.6, 1, and 2 ML, respectively. Comparing these photon energies to the data of Table I the emission is assigned to interband transitions between quantum-well states. Small deviations between the expected transition energies (E_2-E_1) and the measured photon energies are in part due to the electric field of the tip which causes a Stark shift.[38–40] This shift is the strongest for higher-energy states.

Closer inspection reveals a distinct difference of the data from 0.6 and 2 ML compared to the 1-ML case. At 1-ML coverage, a sharp drop on the high-energy side of the emission occurs owing to energy conservation given by the condition $h\nu=eU$. The emission from the 0.6- and 2-ML Na films exhibits a similarly sharp drop at a different energy, $h\nu=eU-E_1$, where E_1 is the energy of quantum-well state 1 relative to the Fermi level.

IV. MODEL AND THEORY

A. General considerations

In this section we will use a rather simple, basically one-dimensional model of the W-tip/Na/Cu(111) system that, nevertheless, captures the essential physics of the experiment and yields calculated spectra that can explain the experimental results.

The general framework of this calculation is based upon what we have used in earlier calculations[18,41] of light emission from noble-metal surfaces. As the more detailed derivation in the Appendix shows, the intensity of the emitted light (per unit photon energy and solid angle) can be calculated from the expression

$$\frac{dP}{d(\hbar\omega)d\Omega}=\frac{2\pi}{\hbar}\sum_{i,f}|j_{fi}|^2\frac{|G(\omega)|^2}{(2\pi)^3}\frac{\hbar\omega^2}{2\epsilon_0 c^3}\delta(E_i-E_f-\hbar\omega). \tag{1}$$

Thus, the intensity is found from a summation over filled initial electron states i and empty final states f, and j_{fi} is the current matrix element between these states,

$$j_{fi}=\frac{-ie\hbar}{2m}\int d^3r\left[\frac{\partial\psi_f^*}{\partial z}\psi_i-\psi_f^*\frac{\partial\psi_i}{\partial z}\right]. \tag{2}$$

In Eq. (1), ϵ_0 is the permittivity of vacuum and c is the speed of light, and G, finally, is an electromagnetic enhancement factor. Note that Eq. (1) agrees with Eqs. (6) and (7) of Ref. 41, considering that the formulas in that work employed cgs units.

Since the calculation of $G(\omega)$ in Eq. (1) has been treated in earlier papers (see, for example, Ref. 42) we will just give a brief outline of the procedure here. As discussed in the Appendix, a reciprocity relation makes it possible to interchange the source and detection points in the electromagnetic calculation. Thus, since we are interested in evaluating the light-emission intensity found at an observation angle $\theta=1$ rad, we let an incident electromagnetic wave hit the tip-sample system from exactly that direction and calculate the electric-field enhancement at a point between the tip apex and the surface, where it reaches its highest values. The field in the cavity between the tip and sample is essentially constant along the direction normal to the surface, however, in the lateral direction the field enhancement begins to drop off at distances exceeding 2–3 nm from the symmetry axis. The optical properties of tip and sample are modeled using macroscopic dielectric functions for Cu and W found from Ref. 43. We have approximated the optical properties of the Na layer by the Cu dielectric function since the treatment of such a thin layer in terms of macroscopic dielectric functions would not be very reliable.[44] The tip is represented by a sphere with radius $R=30$ nm.

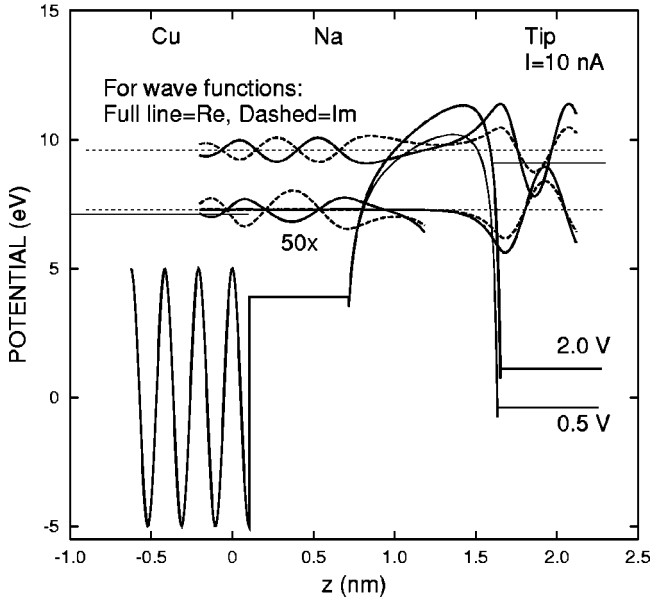

FIG. 3. Illustration of the model potential at two different values of the bias voltage. In addition the wave functions corresponding to the two quantum-well states have been calculated using boundary conditions corresponding to an electron impinging on the barrier from the tip side when $U=2$ V. Note that the wave function at the QWS2 energy penetrates the barrier with high probability, however, since this energy here lies above the tip Fermi energy, this does not contribute to the tunnel current.

B. Model potential

We use a one-dimensional model potential, illustrated in Fig. 3, to calculate both the tunneling current and the matrix elements that set the light-emission rate. The parameter values that enter this model originate from the physical properties of bulk Cu and bulk Na that are most relevant to the problem at hand. Similar models have been used in earlier calculations[45,46] (see also Ref. 47).

Of course, using a strictly one-dimensional (1D) model corresponds to a situation where both electrodes, sample and tip, are completely flat. This is not the real situation in a STM experiment. Thus, we use the 1D model to calculate a current density which then multiplied by a suitable effective area yields the tunnel current. A similar procedure is applied for the matrix-element calculations as well.

Inside the copper sample the potential is modulated along the (111) direction (normal to the surface) as

$$V_{\mathrm{Cu}}(z)=V_{111}(e^{igz}+e^{-igz})=2\,V_{111}\cos(gz), \tag{3}$$

where the reciprocal lattice wave vector $g=2\pi/a_{\mathrm{Cu}}$, and $a_{\mathrm{Cu}}=2.08$ Å is the interplane distance in Cu in the (111) direction. The top layer is centered at $z=0$, and the copper sample is assumed to end at $z=z_{\mathrm{Cu}}=a_{\mathrm{Cu}}/2$. The value of V_{111} is taken to be 2.5 eV.[46] The potential in Eq. (3) yields a band gap for energies (related to electron motion in the z direction) between E_g-V_{111} and E_g+V_{111}, where $E_g=\hbar^2(g/2)^2/(2m)\approx 8.7$ eV is the kinetic energy of a free electron with a wave vector at the L point on the Brillouin-zone boundary. Thus, just as in copper our model has a 5-eV wide band gap at the L point. This feature is crucial in forming quantum-well states in the overlayer system. Experimentally, the energy difference between the lower band edge and the Fermi level is 0.9 eV, we therefore put the Cu Fermi level at $E_F=E_g-V_{111}+0.9\mathrm{eV}=7.1$ eV.

We treat the sodium overlayer as a bulk, free-electron metal. The thickness is assumed to correspond to 2 ML (6.13 Å).[46] The constant value of the potential in the sodium is set to $V_{\mathrm{Na}}=3.9$ eV. The choice of this value is based on the fact that the Fermi energy of bulk Na is 3.2 eV, so that now an electron with the kinetic energy of 3.2 eV in the Na layer will have a total energy of $(3.9+3.2)$ eV$=7.1$ eV, i.e., identical to E_F.

Moreover, in order to get a tunnel current from electrons with energies in the Cu band gap, it is necessary to add a negative imaginary part to the potential. We have chosen to put this in the sodium layer, thus the full Na potential is

$$V_{\mathrm{Na}}-i\Gamma \quad \text{with} \quad \Gamma=0.1 \ \text{eV}.$$

Γ in an approximate way represents the effects of electron-phonon, electron-electron, and interface scattering, which in the real system eventually remove electrons from the quantum-well states near the surface. If the potential had this value in all of space, the electron density due to a particular state would decay in time as $e^{-2\Gamma t/\hbar}$. Thus the lifetime would be $\tau=\hbar/(2\Gamma)\approx 3$ fs, and the peak in the spectral function associated with the state would have a full width at half maximum of 2Γ. It must be kept in mind that an electron in a QWS only spends part of the time ($\approx 50\%$ for QWS1) in the Na layer. Our choice for Γ would thus give a lifetime of some 6 fs, and a line width of 0.1 eV for QWS1. These values are comparable with measured values found in the literature.[48]

We have for simplicity assumed that the potential is constant in the W tip. This is of course a rather crude approximation, but not a crucial one since the electronic structure of the tip is not of primary importance for the analysis of the experiment at hand. With the free-electron bandwidth $W=8.0$ eV, the potential in the tungsten tip at zero bias is $V_{\mathrm{tip}}=E_F-W=-0.9$ eV, however, when the tip is biased the potential is given by $V_{\mathrm{tip}}=E_F-W+eU$.

Finally, we need a barrier potential to use in vacuum between the Na overlayer and the tip. This potential essentially consists of two parts: a tilted square barrier and image potential contributions. The tilted square barrier can be written as

$$V_{\mathrm{tilt}}(z)=\frac{z_{\mathrm{tip}}-z}{d}(E_F+\phi_{\mathrm{Na}})+\frac{z-z_{\mathrm{Na}}}{d}(E_F+eU+\phi_{\mathrm{tip}}), \tag{4}$$

where z_{tip} is the coordinate of the tip apex, z_{Na} is the coordinate of the Na overlayer surface, and d is the tip-sample separation. Here, $\phi_{\mathrm{Na}}=2.7$ eV and $\phi_{\mathrm{tip}}=5.2$ eV denote the Na and tip work functions, respectively, and U is the bias voltage. The image contributions are

$$V_{\mathrm{im}}(z)=-\frac{e^2}{4\pi\epsilon_0 4(z-z_{\mathrm{Na}}^{im})}-\frac{e^2}{4\pi\epsilon_0 4(z_{\mathrm{tip}}^{im}-z)}. \tag{5}$$

We have chosen the image plane position as

$$z_{\mathrm{Na}}^{im}-z_{\mathrm{Na}}=-e^2/[16\pi\epsilon_0(\phi_{\mathrm{Na}}+E_F-V_{\mathrm{Na}})] \tag{6}$$

in the sample. This guarantees that the total potential $V_{\mathrm{tilt}}+V_{\mathrm{im}}$ equals V_{Na}, the potential inside Na, at $z=z_{\mathrm{Na}}$ provided the tip is far away. In the tip, following the same reasoning,

$$z_{\mathrm{tip}}^{im}-z_{\mathrm{tip}}=e^2/[16\pi\epsilon_0(\phi_{\mathrm{tip}}+W)]. \tag{7}$$

The resulting potential is illustrated in Fig. 3 for two different values of the bias voltage.

The model potential described above yields an electronic structure of the Na overlayer, which is in reasonable agreement with experimental observations. In particular, using this model we are able to reproduce the essential features found in the experiment by Hoffmann, Kliewer, and Berndt.[14] At the same time it should be pointed out that the model is not detailed enough to reproduce exactly the same energy-level positions as found experimentally. Given that the Na layer is modeled using bulk parameters, the theoretical results should be more accurate for thicker overlayers. We have therefore concentrated on calculating results for the 2-ML case.

C. Wave functions

To calculate the tunnel current and subsequently the light-emission intensity we must solve the Schrödinger equation for the electron wave functions. Since we have chosen to work with a potential that is translationally invariant in the directions perpendicular to the tunneling direction, we can write all wave functions in the form

$$\psi(\mathbf{r})=\psi(z)e^{i\mathbf{k}_{\parallel}\cdot\mathbf{r}_{\parallel}}. \tag{8}$$

In the copper sample, in view of the potential given by Eq. (3), we make the nearly-free electron model ansatz

$$\psi(z)=\alpha e^{ikz}+\beta e^{i(k-g)z} \tag{9}$$

for the wave function. Inserting this into the Schrödinger equation one finds that there is a band gap for energies (related to the motion in the z direction) between E_g-V_{111} and E_g+V_{111}. In this energy interval there are no bulk states in the copper, however, one can still have surface states for which $k=p-iq$ with $p=g/2$, and

$$q=\sqrt{2m[(4\varepsilon E_g+V_{111}^2)^{1/2}-E_g-\varepsilon]}/\hbar.$$

Thus, the wave-function envelope decays exponentially as e^{qz} and the electron is confined to the region near the copper surface. Since we use a positive value for the corrugation of the potential ($V_{111}=2.5$ eV) states near the bottom of the gap will be *p*-like, whereas states near the top of the gap are *s*-like.[45]

The wave function in Na takes the form

$$\psi(z)=Ae^{ik_{\mathrm{Na}}z}+Be^{-ik_{\mathrm{Na}}z}, \tag{10}$$

where $k_{\mathrm{Na}}=\sqrt{2m(\varepsilon-V_{\mathrm{Na}}+i\Gamma)}/\hbar$ and the branch cut of the square-root function is placed along the negative real axis so that the imaginary part of k_{Na} is positive. In the barrier region, the wave function must be integrated numerically and then joined to the tip wave function

$$\psi(z)=Ce^{ik_{\mathrm{tip}}z}+Fe^{-ik_{\mathrm{tip}}z}, \tag{11}$$

[with $k_{\mathrm{tip}}=\sqrt{2m(\varepsilon-V_{\mathrm{tip}})}/\hbar$] at $z=z_{\mathrm{tip}}$. The coefficients C and F, as well as A and B in Eq. (10), must be determined by wave-function matching.

D. Tunnel current

Before we can evaluate the matrix elements entering Eq. (1) we have to calculate the tunnel current I_{dc}, or rather, determine the tip-sample separation d that yields a certain, set value for I_{dc}. The probability current density in the z direction associated with one particular wave function can be written as

$$j_\psi=\frac{1}{A_{\mathrm{eff}}L}\frac{1}{|F|^2}\mathrm{Re}\left[\psi^*(z)\frac{\hat{p}_z}{m}\psi(z)\right]. \tag{12}$$

Here the first two factors serve as normalization. A_{eff} is the effective area of the tunnel contact, which we also use as a normalization area for the wave functions,[49] L is a normalization length (in the tip), and by dividing by $|F|^2$ we normalize the current to the current carried by the wave impinging on the barrier from the tip side. For a real-valued potential, the probability current j_ψ is independent of the z coordinate. In the present case, with a potential that has a nonzero imaginary part in the sodium layer, the probability current is independent of z to the right (in the barrier and tip) of the Na layer, and can be evaluated anywhere in that part of space. j_ψ vanishes, on the other hand, in the copper since we cannot have any propagating states in the energy gap there. A tunnel current is flowing across the tunnel gap only because of the scattering processes that eventually scatter electrons out of the quantum-well states confined to the Na overlayer and surface region of the copper.

The total electric current is obtained by summing over all contributing states to get a total current density and then multiply by the electron charge and the effective tunneling area,

$$I_{\mathrm{dc}}=-eA_{\mathrm{eff}}\sum_\psi j_\psi. \tag{13}$$

This sum can then be turned into an energy integral.

E. Intensity of emitted light

To calculate the differential power of the emitted light we must carry out the sum over initial and final electron states as indicated in Eq. (1). In contrast to the case of light emission from noble metals the final electron state is in this case, at least in one sense, discrete. Light is primarily emitted while the electron traverses the vacuum barrier and then QWS1 is in practice the only possible final state (assuming parallel momentum is conserved); it dominates the local density of states completely in the energy range just above the substrate Fermi level.

Therefore in the calculations, we have solved for a bound state to represent ψ_f. This state is calculated with essentially the same potential as was used for the tunnel current calculation, however, in this case we set Γ equal to zero, and determine an energy eigenvalue by requiring that the wave function is decaying well inside the tunnel barrier. In the x and y directions this bound-state wave function is assumed to behave like a plane-wave state with a certain momentum. Furthermore, in the following we will assume that this state is almost always unoccupied so that the tunneling electrons can make inelastic transitions into it and emit light at the same time. This last assumption is reasonable because even if most of the tunnel current passes via QWS1, the lifetime of this state is of the order 10^{-14} s while with a tunnel current of 10 nA the delay between each tunnel event is 1.6×10^{-11} s.

In our one-dimensional model the momentum parallel to the interfaces and the electron spin is conserved in the inelastic tunneling process. The sum over initial and final states in Eq. (1) then reduces to integrals over parallel and perpendicular momentum,

$$\begin{aligned}\frac{dP}{d(\hbar\omega)d\Omega}&=\frac{\omega^2|G(\omega)|^2}{8\pi^2\epsilon_0c^3}\sum_{i,f}|j_{fi}|^2\delta(E_i-E_f-\hbar\omega)\\&=2\frac{\omega^2|G(\omega)|^2}{8\pi^2\epsilon_0c^3}A_{\mathrm{eff}}L\int\frac{dk_z}{2\pi}\int\frac{d^2k_\parallel}{(2\pi)^2}|j_{fi}|^2\\&\quad\times\delta(E_i-E_f-\hbar\omega).\end{aligned} \tag{14}$$

Here the integration over parallel momentum can be turned into an energy integration over an interval starting at zero and ending at the maximum energy $E_{\parallel,\max}$ that the electron can have due to the motion parallel to the interfaces. This energy is given by the *tip* Fermi energy, i.e., E_F+eU minus the z motion energy $E_f+\hbar\omega$ in the initial state, i.e., $E_{\parallel,\max}=E_F+eU-E_f-\hbar\omega$. We then get

$$\begin{aligned}\frac{dP}{d(\hbar\omega)d\Omega}&=2\frac{\omega^2|G(\omega)|^2}{8\pi^2\epsilon_0c^3}A_{\mathrm{eff}}L\frac{mE_{\parallel,\max}\Theta(E_{\parallel,\max})}{2\pi\hbar^2}\\&\quad\times\int\frac{dk_z}{2\pi}|j_{fi}|^2\delta(E_i-E_f-\hbar\omega),\end{aligned} \tag{15}$$

where Θ denotes a step function. It remains to carry out the k_z integration, and also this is, in view of the δ function in

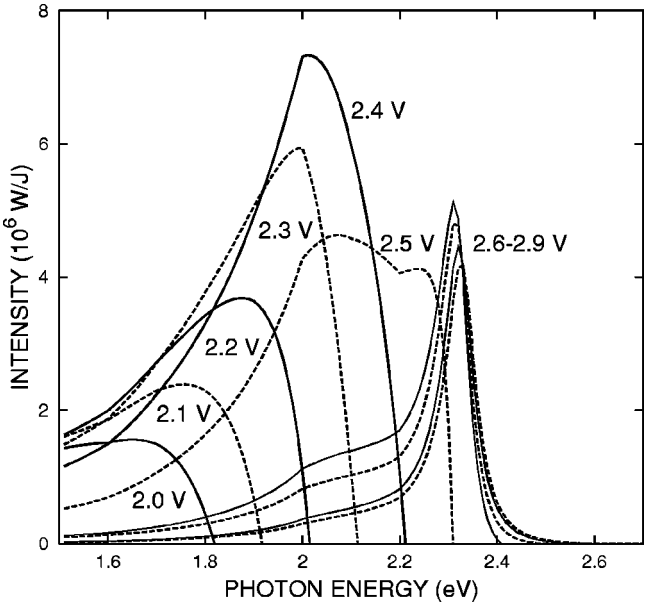

FIG. 4. Calculated light-emission spectra for the Na/Cu(111) system with an overlayer thickness corresponding to 2 ML. The spectra were calculated for a series of bias voltages, while the tunnel current was kept fixed at 10 nA by varying the distance between tip and sample.

the integrand, straightforward. If we let E_b stand for the band bottom energy in the tip, one has $\hbar^2 k_z^2/(2m) = E_i - E_b$. It is then possible to show that

$$\delta(E_i - E_f - \hbar\omega) = \frac{\delta(k_z + \sqrt{2m(E_f + \hbar\omega - E_b)/\hbar^2})}{\frac{\hbar}{m}\sqrt{2m(E_f + \hbar\omega - E_b)}}, \tag{16}$$

and when this is inserted into Eq. (15) we get the final result

$$\frac{dP}{d(\hbar\omega)d\Omega} = A_{\text{eff}} \frac{e^2\omega^2 |G(\omega)|^2}{64\pi^4 \epsilon_0 \hbar c^3} \times \frac{(E_F + eU - E_1 - \hbar\omega)\Theta(E_F + eU - E_1 - \hbar\omega)}{\sqrt{2m(E_1 + \hbar\omega - E_b)}} \times \left| \int dz \left[\frac{\partial \psi_f^*}{\partial z} \psi_i - \psi_f^* \frac{\partial \psi_i}{\partial z} \right] \right|^2. \tag{17}$$

Note that we have made the replacement $E_f \rightarrow E_1$ in the last equation because the final state here is identical to the lowest QWS. The z integration is limited to the vacuum part of space, since the electromagnetic field enhancement is much higher there than in the tip and sample.

V. RESULTS AND DISCUSSION

Figure 4 shows spectra calculated from the model of Sec. IV for a number of different bias voltages. The calculated tunnel current was kept constant at $I_{\text{dc}} = 10$ nA in all cases by changing the tip-sample separation.

We see that these spectra have a number of general qualitative features in common with the experimental spectra shown in Figs. 1 and 2. At first, for bias voltages <2.5 V, the spectrum has a relatively broad peak that is cutoff on the high-energy side. Since QWS1 is the final state in the light-emission process the maximum photon energy equals $eU - (E_1 - E_F)$, and not eU [cf. Eq. (17)].

Once the bias voltage becomes high enough that electrons can be injected into the upper QWS most of the tunnel current will take this path. At the same time the tip-sample separation increases to maintain the tunnel current at a constant value. Quite naturally the electrons injected into the upper QWS will also dominate the light-emission processes at these higher voltages. Most of the emitted photons will have an energy closely corresponding to the energy difference between the two quantum-well states.

Returning to the model, these facts can be understood as follows. As long as the tip Fermi energy lies below QWS2 all initial-state wave functions will decrease exponentially upon traversing the tunnel barrier. Therefore wave functions ψ_i, corresponding to a broad range of energies give comparable contributions to the integral in Eq. (17). The shape of the spectrum in this case is mainly determined by the phase-space factor $(E_F + eU - E_1 - \hbar\omega)$ and the field-enhancement factor $|G(\omega)|^2$.

For higher bias voltages, when $E_F + eU$ exceeds E_2, it is instead the last factor in Eq. (17), the matrix-element integral, that determines the spectral shape. The final state remains the same and therefore, to have a large matrix element, the initial-state wave function ψ_i must be large in the part of space where the final state resides. This will happen when the initial-state energy coincides with E_2 since then *resonant tunneling* into QWS2 is possible and ψ_i will look like the upper wave function illustrated in Fig. 3. Even if there are plenty of initial states with energies both somewhat below and above E_2, they will not at all give as large contributions to the emitted light intensity because their wave functions are much smaller near the Na overlayer surface. As a result of this the light-emission spectrum develops a peak around $h\nu = \hbar\omega = E_2 - E_1$.

The overall intensity of the emitted light is smaller at the higher voltages. The main reason for this is that raising the voltage moves the peak of the light-emission spectrum away from the frequency range near 2 eV where a tungsten tip and a copper sample have an interface-plasmon resonance causing resonantly enhanced light emission. At a photon energy of 2.3–2.4 eV there is still a considerable field enhancement between the tip and sample, but G is typically down by a factor of 2 compared with the resonant case. Thus, the peak in the light-emission spectrum at $h\nu \approx 2.3$ eV is entirely due to the special electron structure of the Na/Cu(111) surface.

The experimental results also illustrate the last point in an interesting way. With 1-ML coverage [Figs. 1 and 2(b)] the emission peak due to quantum-well (or interband) transitions falls at a high photon energy where the electromagnetic enhancement is relatively small. Consequently, comparing spectra taken at different voltages, the plasmon-mediated light emission yields the more intense peaks in these spectra. However, for 0.6-ML coverage [Fig. 2(a)] the quantum-well transition occurs at a lower photon energy, near the maxi-

mum of the electromagnetic enhancement. In this case the ''quantum-well peak'' is more intense than the peak occurring at the lower bias voltage.

In this context let us discuss why it is reasonable to calculate the electromagnetic enhancement at a point just below the tip apex both for plasmon-mediated and QWS transition light emission. In the first case, this is natural since the light-emission event must take place while the electron tunnels from tip to sample. In the latter case, the electron is injected into a fairly long-lived state, and in principle it may end up in a point quite far away from the tip apex before a photon is emitted. However, with a lifetime of 10 fs and a lateral electron velocity of 10^5 m/s the distance traveled by the electron is no more than 1 nm, thus it would still be in a region where the electromagnetic enhancement has not dropped off very much (cf. the discussion in Sec. IV A).

From the calculated results, one can estimate the quantum efficiency of the light-emission process to be 10^{-5} emitted photons per tunneling electron. This number compares well with the experimental result. It is considerably larger than what is observed for inverse photoemission processes at a single surface, however, the quantum efficiency of STM-induced light emission from most notably Ag samples may reach values between 10^{-4} and 10^{-3}.

VI. SUMMARY

In summary we have interpreted experimental observations of STM-induced light emission from the quantum-well system Na on Cu(111) using model calculations of the electronic structure and the optical properties of the tip-sample region. The main features of the experimental data, namely, two distinct spectral structures, and their intensity variation with the tip-sample voltage are reproduced by the calculations. The emission lines are attributed to (a) emission from a localized plasmon which is excited by inelastic tunneling to a quantum-well state and (b) transitions between two quantum-well states. The electromagnetic enhancement present in the tip-sample cavity substantially enhances the intensity of the emission and explains the observed, high quantum efficiencies.

ACKNOWLEDGMENTS

This research was supported by the European Commission via the TMR network *EMIT*. The work of G.H. and R.B. was further supported by the Deutsche Forschungsgemeinschaft via the ''Schwerpunktsprogramm Elektronentransferprozesse an Grenzflächen,'' and the work of P.J. was supported by the Swedish Natural Science Research Council (VR) and by the SSF through the Nanometer Consortium at Lund University.

APPENDIX

In this appendix we derive Eq. (1) using the Keldysh nonequilibrium Green's-function (GF) technique.[50,51] We wish to calculate the intensity of the spontaneously emitted light at a detection point $\mathbf{r}_0$ far away from the STM tip and sample. Since all photons appearing at this point that are of interest to us originate from the region around the STM tip, the intensity can be found by multiplying the electromagnetic energy density, excluding the zero-point energy, by the speed of light. The energy density can be expressed in terms of Keldysh GF's as

$$\mathrm{w}=i\epsilon_0\int_0^\infty \frac{d\omega}{2\pi}[D_{EE}^{<}(\mathbf{r}_0,\mathbf{r}_0,+\omega)+D_{EE}^{>}(\mathbf{r}_0,\mathbf{r}_0,-\omega)], \tag{A1}$$

where $D_{EE}^{<}(\mathbf{r}_0,\mathbf{r}_0,\omega)$ and $D_{EE}^{>}(\mathbf{r}_0,\mathbf{r}_0,\omega)$ are the Fourier transforms of

$$D_{EE}^{<}(\mathbf{r}_0,\mathbf{r}_0,t)=-i\langle E_\theta(\mathbf{r}_0,0)E_\theta(\mathbf{r}_0,t)\rangle \tag{A2}$$

and

$$D_{EE}^{>}(\mathbf{r}_0,\mathbf{r}_0,t)=-i\langle E_\theta(\mathbf{r}_0,t)E_\theta(\mathbf{r}_0,0)\rangle, \tag{A3}$$

respectively. In writing these expressions we have assumed that the tunnel current causing light-emission flows in the z direction near the origin and sends out p-polarized light with an electric field $\mathbf{E}=\hat{\theta}E_\theta$, pointing in the θ direction in the far field. Consequently, the radiated differential power can be written as

$$\frac{dP}{d(\hbar\omega)d\Omega}=\frac{ic\epsilon_0 r_0^2}{2\pi\hbar}[D_{EE}^{<}(\mathbf{r}_0,\mathbf{r}_0,+\omega)+D_{EE}^{>}(\mathbf{r}_0,\mathbf{r}_0,-\omega)]. \tag{A4}$$

The two Keldysh GF's in Eq. (A4) actually yield identical contributions and in the following we will only deal with $D^{<}$.

We need to find an expression for the contributions to $D_{EE}^{<}$, which result from interactions between the electromagnetic field and the electron system in the STM tip and sample. This interaction is to the lowest order

$$H'=\frac{e}{2m}\sum_n [\mathbf{A}(\mathbf{r}_n)\cdot\mathbf{p}_n+\mathbf{p}_n\cdot\mathbf{A}(\mathbf{r}_n)], \tag{A5}$$

where $\mathbf{A}$ is the electromagnetic vector potential ($\mathbf{E}=-\partial\mathbf{A}/\partial t$), the sum runs over the electrons, and $\mathbf{r}_n$ and $\mathbf{p}_n$ are the electron coordinates and momentum operators, respectively. By performing a S-matrix expansion of $D_{EE}^{<}$ to second order in H' we find, using the rules for ''analytic continuation,''[51] that $D_{EE}^{<}$ can be expressed as a product of two photon Green's functions and a current-current Green's function,

$$D_{EE}^{<}(\mathbf{r}_0,\mathbf{r}_0,\omega)=\frac{1}{\hbar^2}\int d^3r_1\int d^3r_2 D_{EA}^{r}(\mathbf{r}_0,\mathbf{r}_1,\omega)\times\Pi^{<}(\mathbf{r}_1,\mathbf{r}_2,\omega)D_{AE}^{a}(\mathbf{r}_2,\mathbf{r}_0,\omega). \tag{A6}$$

These Green's functions are the Fourier transforms of a retarded photon GF

$$D_{EA}^{r}(\mathbf{r},\mathbf{r}',t)=-i\theta(t)\langle[E_\theta(\mathbf{r},t),A_z(\mathbf{r}',0)]\rangle, \tag{A7}$$

an advanced photon GF

$$D^a_{AE}(\mathbf{r},\mathbf{r}',t)=i\theta(-t)\langle[A_z(\mathbf{r},t),E_\theta(\mathbf{r}',0)]\rangle, \quad \text{(A8)}$$

and the current-current GF

$$\Pi^<(\mathbf{r},\mathbf{r}',t)=-i\langle j_z(\mathbf{r}',0)j_z(\mathbf{r},t)\rangle. \quad \text{(A9)}$$

The current-density operator

$$j_z(\mathbf{r})=\frac{-ie\hbar}{2m}\left[\Psi^\dagger(\mathbf{r})\frac{\partial\Psi(\mathbf{r})}{\partial z}-\Psi(\mathbf{r})\frac{\partial\Psi^\dagger(\mathbf{r})}{\partial z}\right], \quad \text{(A10)}$$

where Ψ and $\Psi^\dagger$ are electron annihilation and creation operators.[52]

At this point we can make a number of approximations and simplifications. The inelastic tunneling events occur in a very small part of space in the tunnel gap in a region of (sub) nanometer size. The photon Green's functions do not vary very much on this length scale, so D^r and D^a can be taken outside the integral, and $\mathbf{r}_1$ and $\mathbf{r}_2$ can be replaced by a fixed point $\mathbf{r}_s$ in the tunnel gap in these functions. Fourier transformation turns time derivatives into frequency multiplications. Therefore the photon Green's functions only need to involve the vector potential. Moreover, in Fourier space retarded and advanced GF's are each other's complex conjugates, and finally the reciprocity theorem of electrodynamics allows us to interchange the source and field points in the retarded photon GF. This gives us

$$D^r_{EA}(\mathbf{r}_0,\mathbf{r}_s,\omega)D^a_{AE}(\mathbf{r}_s,\mathbf{r}_0,\omega)=\omega^2|D^r_{z\theta}(\mathbf{r}_s,\mathbf{r}_0,\omega)|^2. \quad \text{(A11)}$$

In a case where parts of space are filled with materials characterized by a relative dielectric function $\epsilon_r(\mathbf{r})$ the (tensor) photon Green's function $D_{\alpha\beta}$ solves[50,53]

$$\left[\nabla\times\nabla\times-\epsilon_r(\mathbf{r})\frac{\omega^2}{c^2}\right]D^r_{\alpha\beta}(\mathbf{r},\mathbf{r}',\omega)=-\hbar\mu_0\hat{\beta}\delta^3(\mathbf{r}-\mathbf{r}') \quad \text{(A12)}$$

and yields the α component of the vector potential in the point $\mathbf{r}$ if there is a δ function current source pointing in the β direction in $\mathbf{r}'$. Thus, $D^r_{\alpha\beta}(\mathbf{r},\mathbf{r}',\omega)$ can be calculated within the framework of classical electrodynamics. The $z\theta$ element of interest here can be written as

$$D^r_{z\theta}(\mathbf{r}_s,\mathbf{r}_0,\omega)=-\frac{\hbar}{\epsilon_0c^2}\frac{e^{ikr_0}}{4\pi r_0}G(\theta_0,\omega), \quad \text{(A13)}$$

where G is an enhancement amplitude. G is given by the z component of the local electric field in the tunnel gap when a plane wave of unit amplitude incident from the direction of $\mathbf{r}_0$ impinges on the tip-sample system. In free space one would simply have $G(\theta,\omega)=\sin\theta$. The detailed scheme for calculating G has been described earlier, for example, in Ref. 42.

It remains to evaluate the current-current Green's function $\Pi^<(\mathbf{r}_1,\mathbf{r}_2,\omega)$ and to carry out the integrations over the coordinates $\mathbf{r}_1$ and $\mathbf{r}_2$ in Eq. (A6). A straightforward evaluation yields the result

$$\int d^3r_1\int d^3r_2\Pi^<(\mathbf{r}_1,\mathbf{r}_2,\omega) = -2\pi i\hbar\sum_{fi}|j_{fi}|^2\delta(\hbar\omega+E_f-E_i), \quad \text{(A14)}$$

where the sum runs over filled initial electron states i with energy E_i and wave function ψ_i and empty final electron states f with energy E_f and wave function ψ_f, and

$$j_{fi}=\frac{-ie\hbar}{2m}\int d^3r\left[\frac{\partial\psi_f^*}{\partial z}\psi_i-\psi_f^*\frac{\partial\psi_i}{\partial z}\right]. \quad \text{(A15)}$$

By inserting the results of Eqs. (A6), (A11), (A13), and (A14) in Eq. (A4) we arrive at the final result

$$\frac{dP}{d(\hbar\omega)d\Omega}=\frac{\omega^2|G(\theta_0,\omega)|^2}{8\pi^2\epsilon_0c^3}\sum_{fi}|j_{fi}|^2\delta(\hbar\omega+E_f-E_i), \quad \text{(A16)}$$

which is identical to Eq. (1).

[1] S.-A. Lindgren and L. Walldén, Solid State Commun. **34**, 671 (1980).
[2] S.-A. Lindgren and L. Walldén, Phys. Rev. Lett. **59**, 3003 (1987).
[3] R.D. Diehl and R. McGrath, Surf. Sci. Rep. **23**, 43 (1996).
[4] C. Stampfl and M. Scheffler, Surf. Rev. Lett. **2**, 317 (1995).
[5] H. Tochihara and S. Mizuno, Prog. Surf. Sci. **48**, 75 (1998).
[6] B. Hellsing, J. Carlsson, L. Walldén, and S.-A. Lindgren, Phys. Rev. B **61**, 2343 (2000).
[7] J.M. Carlsson and B. Hellsing, Phys. Rev. B **61**, 13 973 (2000).
[8] R. Dudde, L.S.O. Johansson, and B. Reihl, Phys. Rev. B **44**, 1198 (1991).
[9] N. Fischer, S. Schuppler, R. Fischer, Th. Fauster, and W. Steinmann, Phys. Rev. B **43**, 14 722 (1991).
[10] A. Carlsson, D. Claesson, S.-A. Lindgren, and L. Walldén, Phys. Rev. Lett. **77**, 346 (1996).
[11] M. Bauer, S. Pawlik, and M. Aeschlimann, Phys. Rev. B **55**, 10 040 (1997).
[12] S. Ogawa, H. Nagano, and H. Petek, Phys. Rev. Lett. **82**, 1931 (1999).
[13] A.G. Borisov, J.P. Gauyacq, A.K. Kazansky, E.V. Chulkov, V.M. Silkin, and P.M. Echenique, Phys. Rev. Lett. **86**, 488 (2001).
[14] G. Hoffmann, J. Kliewer, and R. Berndt, Phys. Rev. Lett. **87**, 176803 (2001).
[15] For a recent review see: R. Berndt, in *Scanning Probe Microscopy*, edited by R. Wiesendanger (Springer, Berlin, 1998), pp. 97–134.
[16] J.K. Gimzewski, B. Reihl, J.H. Coombs, and R.R. Schlitter, Z. Phys. B: Condens. Matter **72**, 497 (1988).
[17] J.K. Gimzewski, J.K. Sass, R.R. Schlitter, and J. Schott, Europhys. Lett. **8**, 435 (1989).
[18] P. Johansson, R. Monreal, and P. Apell, Phys. Rev. B **42**, 9210 (1990).
[19] R. Berndt, J.K. Gimzewski, and P. Johansson, Phys. Rev. Lett. **67**, 3796 (1991).

[20] B.N.J. Persson and A. Baratoff, Phys. Rev. Lett. **68**, 3224 (1992).
[21] Y. Uehara, Y. Kimura, S. Ushioda, and K. Takeuchi, Jpn. J. Appl. Phys., Part 1 **31**, 2465 (1992).
[22] R. Berndt and J.K. Gimzewski, Phys. Rev. B **48**, 4746 (1993).
[23] P. Johansson, Phys. Rev. B **58**, 10 823 (1998).
[24] Y. Uehara, T. Fujita, and S. Ushioda, Phys. Rev. Lett. **83**, 2445 (1999).
[25] N. Nilius, N. Ernst, and H.-J. Freund, Phys. Rev. Lett. **84**, 3994 (2000).
[26] D.L. Abraham, A. Veider, Ch. Schönenberger, H.P. Meier, D.J. Arent, and S.F. Alvarado, Appl. Phys. Lett. **56**, 1564 (1990).
[27] R. Berndt and J.K. Gimzewski, Phys. Rev. B **45**, 14 095 (1992).
[28] C. Thirstrup, M. Sakurai, K. Stokbro, and M. Aono, Phys. Rev. Lett. **82**, 1241 (1999).
[29] S. Kagami, H. Minoda, and N. Yamamato, Surf. Sci. **493**, 78 (2001).
[30] Ph. Renaud and S.F. Alvarado, Phys. Rev. B **44**, 6340 (1991).
[31] J. Lindahl, M.-E. Pistol, L. Montelius, and L. Samuelson, Appl. Phys. Lett. **68**, 60 (1996).
[32] R. Berndt, R. Gaisch, J.K. Gimzewski, B. Reihl, R.R. Schlittler, W.-D. Schneider, and M. Tschudy, Science **262**, 1425 (1993).
[33] G.E. Poirier, Phys. Rev. Lett. **86**, 83 (2001).
[34] J. Kliewer, Ph.D. thesis, RWTH Aachen, Germany (2000).
[35] G. Hoffmann, J. Kröger, and R. Berndt, Rev. Sci. Instrum. **73**, 305 (2002).
[36] D. Tang, D. McIlroy, X. Shi, C. Su, and D. Heskett, Surf. Sci. **255**, L497 (1991).
[37] G. Hoffmann and R. Berndt, Int. J. Nanoscience **1**, 53 (2002).
[38] R.S. Becker, J.A. Golovchenko, and B.S. Swartzentruber, Phys. Rev. Lett. **55**, 987 (1985).
[39] G. Binnig, K.H. Frank, H. Fuchs, N. Garcia, B. Reihl, H. Rohrer, F. Salvan, and A.R. Williams, Phys. Rev. Lett. **55**, 991 (1985).
[40] G. Hoffmann, L. Limot, P. Johansson, and R. Berndt (unpublished).
[41] P. Johansson and R. Monreal, Z. Phys. B: Condens. Matter **84**, 269 (1991).
[42] P. Johansson, S.P. Apell, and D.R. Penn, Phys. Rev. B **64**, 054411 (2001).
[43] E. D. Palik, *Handbook of Optical Constants of Solids* (Academic Press, New York, 1985).
[44] Ideally, the electromagnetic response for a system including a very thin overlayer should be found from a microscopic calculation. For an example, see A. Liebsch, B.-O. Kim, and E.W. Plummer, Phys. Rev. B **63**, 125416 (2001).
[45] N.V. Smith, Phys. Rev. B **32**, 3549 (1985).
[46] S.-A. Lindgren and L. Walldén, Phys. Rev. B **38**, 3060 (1988).
[47] A. Zangwill, *Physics at Surfaces* (Cambridge University Press, Cambridge, 1988), pp. 63–67.
[48] A. Carlsson, B. Hellsing, S.-A. Lindgren, and L. Walldén, Phys. Rev. B **56**, 1593 (1997).
[49] We used an effective area of 8 nm^2 in the calculations. The light-emission results are not very sensitive to the exact value of A_{eff} as long as the tunnel current is kept at a fixed value.
[50] G. D. Mahan, *Many-Particle Physics* (Pergamon, New York, 1990), pp. 117–130.
[51] A.-P. Jauho, N.S. Wingreen, and Y. Meir, Phys. Rev. B **50**, 5528 (1994).
[52] G. Rickayzen, *Green's Functions and Condensed Matter* (Academic Press, London, 1980), p. 344.
[53] E. M. Lifshitz and L. P. Pitaevskii, *Statistical Physics, Part 2* (Butterworth-Heinemann, Oxford, 1999), pp. 314–359.